Talanta 263 (2023) 124693

Contents lists available at ScienceDirect

Talanta

journal homepage: www.elsevier.com/locate/talanta

Determination of endogenous trace elements in extracellular vesicles secreted by an *in vitro* model of human retinal pigment epithelium under oxidative stress conditions using ICP-MS

Jaime Martínez-García [a], Beatriz Fernández [a,*], Ana Álvarez-Barrios [a,b], Lydia Álvarez [b], Héctor González-Iglesias [c,**], Rosario Pereiro [a]

[a] Department of Physical and Analytical Chemistry, University of Oviedo, Julian Clavería 8, 33006, Oviedo, Spain
[b] Fundación de Investigación Oftalmológica, Avda, Dres, Fernández-Vega, 34, 33012, Oviedo, Spain
[c] Dairy Research Institute of Asturias, Spanish National Research Council (IPLA-CSIC), Villaviciosa, Spain

ARTICLE INFO

Keywords:
Exosomes
Retinal pigment epithelial cells
Oxidative stress
Zinc
ICP-MS

ABSTRACT

The determination of endogenous Fe, Cu and Zn in exosomes (<200 nm extracellular vesicles) secreted by an *in vitro* model of the human retinal pigment epithelium (HRPEsv cell line) was carried out by inductively coupled plasma - mass spectrometry (ICP-MS). Results for cells treated with 2,2′-azobis (2-methylpropionamidine) dihydrochloride (AAPH) inducing oxidative stress (OS) conditions were compared with non-treated (control) cells in order to evaluate possible differences in the metal composition between both groups. Three sample introduction systems were tested for ICP-MS analysis: a micronebulizer and two single cell nebulization systems (as total consumption set-ups), being found one of the single cell systems (operating in bulk mode) as the most suitable. Two protocols for the isolation of exosomes from cell culture media were investigated based on differential centrifugation and precipitation with a polymer-based reagent. Transmission electron microscopy measurements showed smaller and more homogeneous sizes (15–50 nm *versus* 20–180 nm size range) together with a higher particle concentration for exosomes purified by precipitation compared to differential centrifugation. However, it was observed that the contribution of polymer-based protocol to the Fe, Cu and Zn blank was significant as compared to the differential centrifugation protocol. Therefore, considering the low concentrations of the evaluated endogenous elements in exosomes from the HRPEsv cell line, the polymer-based precipitation method was discarded. When comparing metal levels in samples from control *versus* OS-treated HRPEsv cells, results for Fe and Cu were statistically similar. However, upregulation of Zn was found during OS conditions (11 *versus* 34 μg L^{-1} in control and OS-treatment, respectively), showing Zn depletion through secretory activity induced by OS, underlying the antioxidant ability of RPE cells.

1. Introduction

Extracellular vesicles (EVs) are cell secreted membranous particles containing DNA, RNA, lipids and proteins, involved in cell-to-cell signaling and cell waste disposal [1–3]. Although different EVs sub-populations are described in the bibliography, there is a lack of homogeneity for their classification [4]. According to biogenesis and size, EVs are typically classified, from smallest to biggest, as exosomes, microvesicles and apoptotic bodies. Exosomes are EVs formed in the cell cytosol with sizes typically below 200 nm, whereas microvesicles are bigger in size (200–1000 nm) and are formed by budding of the cell membrane [5]. Apoptotic bodies can reach up to several microns in size and are formed in the process of programmed cell death by cell fragmentation [6].

EVs have gained popularity in the biomedical research field in the last decade, not only for their potential use as drug-delivery carriers [7], but also for their possible utilization as disease biomarkers [8]. Specifically, exosomes are an EV sub-population with particular promising research interest, as they reflect cellular metabolism, intercellular communication and secretion [9]. Thus, an imbalance in the cell

* Corresponding author.
** Corresponding author.
E-mail addresses: fernandezbeatriz@uniovi.es (B. Fernández), hectorgi@ipla.csic.es (H. González-Iglesias).

https://doi.org/10.1016/j.talanta.2023.124693
Received 30 March 2023; Received in revised form 15 May 2023; Accepted 18 May 2023
Available online 22 May 2023

homeostatic equilibrium may be manifested through cell secretory activity. Recent studies have revealed that secretory activity of cells can be modified when they are exposed to stress stimuli, such as oxidative stress (OS) or inflammation, showing the relationship between secretory activity and inner metabolic activity of cells [10,11]. In particular, the study of the secretory activity of cells under OS conditions is important for specific pathologies, such as cancer and neurodegenerative diseases, as the early forms of such diseases are associated with OS and metabolic dyshomeostasis [12,13].

OS strongly affects the human eye, specifically the cells of the posterior pole, i.e., the neurosensory retina and its retinal pigment epithelium (RPE), which oxidative damage is exacerbated during ageing [14]. RPE is a monolayer of cells that is part of the blood-retina barrier and is the main trafficking channel between retinal cells and the bloodstream for the transport of nutrients and waste disposal [15]. RPE dysfunction induced by OS contribute to the pathogenesis of eye diseases, including age-related macular degeneration (AMD) [16], recently suggesting a tight relationship between RPE secretory activity and AMD disease onset [17,18]. Remarking the importance of the secretory activity in the possible manifestation of metabolic dyshomeostasis induced by OS conditions, previous studies have recently revealed that some of the proteins found in drusen (extracellular deposits in the basal region of the RPE that are a clinical hallmarks of AMD) are also present in exosomes, indicating the tight relationship between secretory activity of the cells and their potential to be used as disease biomarkers [18].

RPE contains a wide variety of antioxidants requiring metals for their activity, including Fe, Cu and Zn [14], therefore, OS induced metabolic dyshomeostasis of RPE cells may alter its secretory activity affecting exosomes metal composition. In this work, the determination of Fe, Cu and Zn in exosomes secreted by an *in vitro* model of RPE cells under control and OS-induced conditions was investigated to study possible differences in their content, because several enzymatic antioxidant enzymes use these elements as cofactors [14]. The lack of standardized methods for EVs isolation together with the low concentration expected of target metals in EVs and the reduced sample volume typically available (below 100 μL) limit the potential analytical techniques for determining endogenous metals in EVs. To our knowledge, there are not published studies related to the determination of endogenous elements in exosomes secreted by a cell line. As it is well known, inductively coupled plasma - mass spectrometry (ICP-MS) allows to determine elemental content in a wide variety of biological matrices with excellent limits of detections [19]. However, the analysis of endogenous metals in EVs has not been reported up to date by ICP-MS and, therefore, their role during exosomes secretion induced by OS remains unexplored.

In our studies, a human RPE cell line (HRPEsv) was used for the establishment of the *in vitro* cellular model and 2,2′-azobis (2-methylpropionamidine) dihydrochloride (AAPH) was employed to achieve OS conditions. Two protocols for exosomes isolation from RPE cell culture media, based on differential centrifugation and precipitation (using the ExoQuick-TC commercial kit), were evaluated in terms of size and number of isolated EVs, as well as concentration of Fe, Cu and Zn. Considering that the analysis of low volume samples is still challenging by ICP-MS, three sample introduction set-ups were investigated for the analysis of exosomes by ICP-MS, including a micronebulizer and two interfaces designed for single cell analysis (as total consumption set-ups).

2. Materials and methods

2.1. Instrumentation

Centrifugation and ultracentrifugation steps for exosomes isolation were respectively performed with 5810 R Centrifuge (Eppendorf SE) and Optima L-90 K Ultracentrifuge (Beckman Coulter, Inc.). TEM images of EVs were acquired with a JEM 1011 Electron Microscope (JEOL Ltd.). Spectrophotometric measurements for total protein and CD81 protein quantification were performed with a Victor^{TM} X5 microplate reader (PerkinElmer).

ICP-MS measurements were carried out with a 7900 series quadrupole ICP-MS (Agilent Technologies). Three sample introduction systems were investigated: (i) MicroMist DC Nebulizer (Glass Expansion), (ii) Single Cell sample introduction system (Glass Expansion) including a MicroMist HE U-Series nebulizer and a single cell chamber, and (iii) microFAST Single Cell system (Elemental Scientific, Inc.) including a CytoNeb nebulizer, a CytoSpray chamber and one-piece ICP-MS torch.

2.2. HRPEsv cell culture conditions and AAPH-induced oxidative stress treatment

A human RPE cell line (HRPEsv) established from a primary culture of RPE cells [20] was cultured with cell proliferation medium i.e., Dulbecco's modified eagle medium/nutrient mixture F-12 (DMEM:F12) (Sigma-Aldrich) supplemented with 1% (v/v) antibiotic-antimycotic solution (1:1 mixture of penicillin:streptomycin, P/S) (Gibco, Thermo-Fischer Scientific) and 10% (v/v) fetal bovine serum (FBS) (Gibco, Thermo-Fischer Scientific). For exosomes collection and characterization, HRPEsv cells were cultured in T75 Corning® flasks with cell proliferation medium till 50–60% confluence. Then, FBS was replaced by 10% (v/v) exosome-depleted FBS (Gibco, Thermo-Fischer Scientific), labeled as exosome-depleted medium, to avoid external exosome contribution. After 72 h, cells reached confluence to finally collect the culture medium containing EVs for further isolation.

For OS treatment, HRPEsv cells were supplemented with AAPH from Acros Organics (Thermo-Fischer Scientific). The AAPH concentration was optimized to induce cellular OS response while ensuring the cells integrity is not compromised. For such purpose, HRPEsv cells were cultured in 96-well microplates ($3{\cdot}10^3$ cells per well) in supplemented DMEM:F12 medium, replaced by Ex-cell® serum-free medium supplemented with 5% (v/v) L-glutamine (Gibco, Thermo-Fischer Scientific) and 1% (v/v) P/S, over 24 h. Then, cells were treated with different concentrations of AAPH (0–100 mM) during 24 h. Cell viability was determined with a CyQuant™ direct cell proliferation assay (Thermo-Fischer Scientific). A microplate reader was employed to measure fluorescence emission with 485 nm/535 nm wavelength excitation/emission filters. A significant decrease in the cell viability for AAPH concentrations higher than 10 mM was observed, selecting a 5 mM AAPH concentration during 24 h for the HRPEsv cells OS-treatment.

2.3. Exosomes isolation and characterization

2.3.1. Isolation of exosomes from HRPEsv cells culture medium

The exosomes were isolated from HRPEsv cell culture media assessing two protocols based either on differential centrifugation or precipitation. For differential centrifugation, a previously reported protocol was first evaluated [21], introducing an additional centrifugation step to remove large microvesicles [22]. Briefly, cells culture medium was subjected to different centrifugation steps to remove unwanted debris prior to exosomes sedimentation, using 38.5 mL open-top thin wall polypropylene ultracentrifuge tubes (Beckman Coulter). The supernatant was collected and the pellet discarded, as follows: 300×*g* 10 min for sedimentation of cells, 2,000×*g* 20 min for sedimentation of cell debris, 10,000×*g* 30 min for large vesicle sedimentation and 40,000×*g* 30 min for microvesicle sedimentation. Clear medium was then submitted to ultracentrifugation for exosomes pelleting at 100,000×*g* 70 min. Finally, a pellet washing step with 1X phosphate buffered saline (PBS, pH 7.4) was done along with another ultracentrifugation step at 100,000×*g* 70 min, allowing to obtain the exosomes pellet. The final pellet was resuspended in 80 μL (minimum volume required for exosomes characterization by TEM, determination of total protein concentration and CD81 exosomes marker, and elemental analysis by ICP-MS) of 1X PBS (pH 7.4) and then filtered through a 0.22 μm syringe filter. All centrifugation and ultracentrifugation steps were carried out at 4 °C.

For precipitation, ExoQuick-TC kit (System Biosciences) containing a polymer-based solution was selected. Two buffers for exosomes resuspension were investigated: 1X PBS and 10 mM tris(hydroxymethyl) aminomethane (Tris) buffer, both at pH 7.4. Manufacturer's protocol was as follows: culture medium samples were cleared by centrifuging them at 3,000×*g* 15 min for cell and cell debris pelleting, and the supernatant was thoroughly mixed 5:1 with ExoQuick-TC reagent and incubated overnight at 4 °C. The resulting mixture was centrifuged at 1,500×*g* 30 min for exosomes pelleting and then the pellet was washed with 1X PBS (pH 7.4) and re-pelleted with another centrifugation step at 1,500×*g* 30 min. The final pellet was resuspended in 80 μL of 1X PBS (pH 7.4). A filtration step using Millex-GV 0.22 μm PVDF filtration units (Merck Millipore) was finally performed.

2.3.2. Characterization of exosomes by TEM

Vesicle-like particles require a specific contrasting treatment for Transmission electron microscopy (TEM) characterization, and different sample preparation protocols can be found in bibliography [23]. Table 1 collects the protocols we have evaluated. These include using 4% (w/v) paraformaldehyde (PFA, Acros Organics, Thermo Fischer Scientific) for exosomes fixation, 2% (w/v) phosphotungstic acid (PTA, Merck) or 2% (w/v) uranyl acetate (UA, Electron Microscopy Sciences) for negative exosomes staining, and 1% (w/v) osmium tetroxide (Electron Microscopy Sciences) for positive exosomes staining. Exosomes were deposited onto formvar/carbon-coated 200-mesh copper grids (Sigma Aldrich) prior to TEM analyses. Additionally, the two buffers at pH 7.4 (1X PBS and 10 mM Tris) were compared to study their compatibility with the sample preparation procedures for the analysis of exosomes.

2.3.3. Total protein concentration in exosomes determined by BCA assay

The total protein content of the samples (exosomes isolated from HRPEsv cells culture medium and procedural blanks) was determined by the bicinchoninic acid assay using a QuantiPro™ BCA assay kit (Sigma-Aldrich) following manufacturer's instructions. All solutions were transferred to a 96-well plate and incubated 1 h at 65 °C. After the incubation, the absorbance of each well was measured at 562 nm wavelength.

2.3.4. CD81 determination in exosomes by ELISA

In order to confirm exosomes presence, a straightforward method using a general exosomes marker like the tetraspanin CD81 was also performed. The levels of CD81 in isolated exosomes samples were determined using a commercial ELISA kit for human CD81 (FineTest, Wuhan Fine Biotech Co.), following manufacturer's instructions. In this case, a total culture medium volume of 180 mL was employed and differential centrifugation was used for exosomes isolation.

2.3.5. EVs isolation from OS-induced treatment

EVs collection protocol followed in the OS-induced treatment was similar than for control (CT) conditions. HRPEsv cells were grown in T75 flasks and culture medium was changed to exosome-depleted medium when cells reached 50–60% confluence. After 48 h of incubation with exosome-depleted medium, a solution with the corresponding AAPH concentration in 1X PBS at pH 7.4 (previously filtered with a 0.22 μm syringe filter) was added directly to the medium. After 24 h of treatment, medium was collected and submitted to exosomes isolation. It must be noted that each sample comes from six T75 Corning® flasks with confluent cells, making a total culture medium volume of 90 mL per sample. In all cases and for each condition (CT and OS-treated) three biological replicates were performed.

Table 1
Sample preparation protocols evaluated for TEM analysis of exosomes isolated from HRPEsv cells culture medium. Each protocol was tested using two different buffers for exosomes resuspension: 1X PBS (pH 7.4) and 10 mM Tris (pH 7.4).

Protocol	Fixation	Post-fixation	Staining
1	–	–	2% Phosphotungstic acid - 1 min in grid
2	–	–	2% Uranyl acetate - 1 min in grid. Avoid light exposure
3	Paraformaldehyde (PFA) 4% - 1 h in solution.	–	2% Uranyl acetate - 7 min in grid. Avoid light exposure
4	Paraformaldehyde (PFA) 4% - 1 h in solution.	1% Osmium tetroxide - 30 min in grid	2% Uranyl acetate - 7 min in grid. Avoid light exposure

2.4. Multielemental analysis by ICP-MS

For ICP-MS measurements, trace metal standards were prepared from 1000 mg L^{-1} standard solution of each metal (Fe, Cu, Zn and Ga, Sigma-Aldrich) in 3% ultrapure HNO_3 (concentrated HNO_3 sub-boiling distillated from LabKem). Chelex-100 resin (Na form, 100–200 dry mesh) from Bio-Rad Laboratories was used to remove Fe, Cu and Zn ions in the buffer used to resuspend isolated exosomes. The resin was first converted to its acid form by treatment with 2 M hydrochloric acid (under mechanical stirring for 2 h) and subsequently was rinsed with ultrapure water to eliminate the excess of acid. Deionized ultrapure water, resistivity 18.2 MΩ cm (Purelab Flex 3&4; ELGA-Veolia, High Wycombe) was utilized throughout.

External calibrations with pure standards for Fe, Cu and Zn were made for ICP-MS analysis (metal concentrations ranging 0–20 μg L^{-1} and containing 10 μg L^{-1} Ga as internal standard; solutions in 3% nitric acid). Specific conditions for ICP-MS measurements using the three sample introduction systems evaluated in this work are collected in Table 2. Before ICP-MS analysis, exosomes resuspended in PBS buffer were diluted 1:2 for differential centrifugation-isolated samples and 1:5 for precipitation-isolated samples (final concentration of 3% nitric acid and 10 μg L^{-1} Ga as internal standard). Calibrations were performed for each particular case using the same buffer than that employed for the sample (calibration performed for precipitation-isolated samples were made in 1X PBS diluted 1:5 to a final concentration of 3% nitric acid and 10 μg L^{-1} Ga, while same procedure was carried out for differential centrifugation-isolated samples but applying a dilution factor of 1:2). Statistical differences in the levels of the investigated metals were evaluated using GraphPad Instat (version 3.10), conducting an unpaired *t*-test (normality tested using the method Shapiro-Wilk).

Table 2
ICP-MS operating conditions for the analysis of trace elements in exosomes from HRPEsv cells culture medium using different sample introduction systems (MicroMist DC nebulizer, the Single Cell system from Glass Expansion, and the microFAST Single Cell system from Elemental Scientific, Inc.).

Acquisition mode	Spectrum
RF power	1550 W
Auxiliary gas	0.9 L min^{-1}
Plasma gas	15 L min^{-1}
Nebulizer gas flow	• MicroMist: 1 L min^{-1} • Single Cell: 0.7 L min^{-1} • microFAST: 0.25 L min^{-1}
Make up gas flow	• MicroMist: 0 L min^{-1} • Single Cell: 0.5 L min^{-1} • microFAST: 0.8 L min^{-1}
Collision-Reaction Cell gas flow	He: 4.4 mL min^{-1} (Fe) H_2: 3.7 mL min^{-1} (Cu and Zn)
Stabilization time	15 s
Integration time	0.1 s
Measured isotopes	^{56}Fe, ^{57}Fe, ^{63}Cu, ^{64}Zn, ^{65}Cu, ^{66}Zn, ^{69}Ga, ^{71}Ga
Nebulizer pump speed	• MicroMist: 0.02 rpm • Single Cell: 0.01 rpm • microFAST: 0.1 rpm

3. Results and discussion

3.1. Characterization of EVs isolated from HRPEsv cells culture medium

As described in the Experimental Section, two isolation protocols were investigated with HRPEsv cells culture medium. In both cases a total culture medium volume of 90 mL was employed. Additionally, different sample preparation strategies were evaluated to get high quality images from isolated EVs by TEM (described in Table 1). TEM images of EVs isolated by differential centrifugation using PBS and Tris buffers are respectively collected in Fig. S1 and Fig. S2 in the Supporting Information. Similarities for EVs images acquired by staining with phosphotungstic acid (Protocol 1 – Table 1) were observed with both buffers (Figs. S1A and S2A): spherical black particles were detected with stains surrounding them, suggesting that the staining agent covers EVs heterogeneously. For images acquired using Protocol 2 in PBS (Fig. S1B) and Protocol 4 in Tris (Fig. S2D), crystal formation was observed: geometrically shaped structures were detected instead of particle-like structures. Such protocols were discarded for TEM measurements of isolated-EVs. The rest of the sample preparation protocols provided well contrasted images of EVs. In any case, images of EVs obtained using the Protocol 2 in PBS (Fig. S1C) showed the best contrast and this buffer was selected for further experiments.

For comparison, Fig. 1 shows TEM images obtained using the selected optimized protocol (fixation with 4% PFA (w/v) and staining with 2% uranyl acetate (w/v)) for EVs isolated by precipitation (Fig. 1A) and differential centrifugation (Fig. 1B) of the culture medium from confluent HRPEsv cells using a 200000× magnification. Particles with a dark edge and a lighter inner part can be seen in both cases, which agrees with the term "cup-shaped" previously described for exosomes [24], indicating that exosomes were successfully isolated from HRPEsv cells culture medium both by differential centrifugation and precipitation.

Concerning the image obtained by using the differential centrifugation protocol (Fig. 1B), exosomes together with some aggregates can be observed, that is typical from such isolation protocol: it has been reported that the extremely high centrifugal forces employed can induce EVs aggregation [25]. Additionally, procedural blanks were prepared using the ExoQuick-TC reagent (precipitation) or PBS (differential centrifugation) together with the culture medium with the absence of HRPEsv cells. Fig. 1C collects the image obtained for the procedural blank using the precipitation protocol to evaluate by TEM the possible contribution of ExoQuick-TC reagent, which is a polymer-based solution and could interfere in EVs images. As can be observed, particles with exosomes characteristics were not observed for the ExoQuick blank. In the case of differential centrifugation isolation protocol, blank contribution was also negligible (1X PBS pH 7.4, data not shown).

Concerning the size of the isolated exosomes, the particle size distribution obtained for the two purification protocols has been estimated from TEM images. As an example, Fig. 2 shows the typical histograms obtained for the exosomes isolated by precipitation (Fig. 2A) and differential centrifugation (Fig. 2B) in terms of number of vesicles per range size. Such histograms correspond to the TEM images collected in Fig. 1. In the histograms, the term size was considered as the longer diameter of the exosomes detected (in the sample preparation protocol the vesicle shape can be distorted and most of the exosomes acquire an oval rather than spherical shape [26]). Experimental results showed a higher number of vesicles using the precipitation protocol compared to differential centrifugation: the average density (the number of exosomes per μm^2 grid) was found to be 585, 511 and 475 exosomes μm^{-2} using the precipitation protocol, whereas 18, 16 and 15 exosomes μm^{-2} was obtained by using differential centrifugation (three biological replicates in each case). Additionally, as can be seen in Figs. 1 and 2, the size of exosomes isolated by precipitation was significantly smaller (below 50 nm) than that obtained by differential centrifugation (up to 180 nm). This last also exhibited a higher size polydispersity in the range of 20–180 nm (compared to 15–50 nm range for precipitation). Exosomes isolated by differential centrifugation were also identified by using an ELISA assay for CD81. Experimental results showed a concentration of 3.51 μg L^{-1} of CD81 in the isolated exosomes.

The total protein content was determined in exosomes suspensions, showing a significant difference for the two isolation protocols investigated: 641 ± 188 mg L^{-1} for precipitation and 19 ± 5 mg L^{-1} for differential centrifugation (standard deviation from the mean of three biological replicates). Thus, experimental results confirm a better isolation efficiency by precipitation compared to differential centrifugation protocol.

3.2. Determination of trace elements in exosomes by ICP-MS

3.2.1. Optimization of the experimental conditions

After isolation of exosomes from HRPEsv cells culture medium by precipitation or differential centrifugation, they were resuspended using a saline buffer. PBS is used as the standard buffer in almost all EVs-related works as it maintains EVs integrity due to its salt content. However, the main limitation of buffers used for ICP-MS analysis is related to metal impurities, because salts used for preparation are not ultratrace-metals grade. As proteins have been the main target analytes studied in EVs, no special attention was paid up to date to contamination related to the buffer employed for EVs resuspension. Two buffers were evaluated in this work to ensure exosomes stability and suitability for metals determination by ICP-MS: 1X PBS pH 7.4 and 10 mM Tris pH 7.4. Tris has not been widely proposed for EVs analysis but is a commonly used buffer for biological samples' dilution and resuspension. As can be seen in Fig. 3, the Cu content was similar in PBS and Tris buffers, whereas Fe and Zn levels detected in Tris were significantly higher

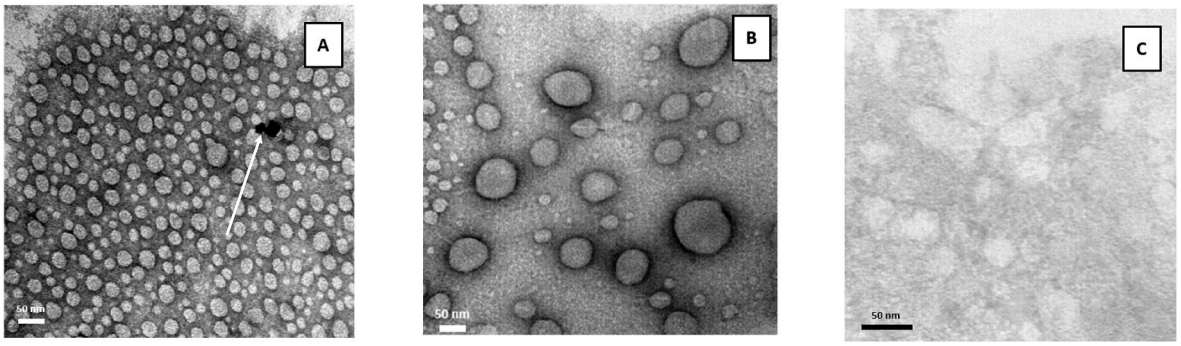

Fig. 1. Images obtained by TEM for the characterization of EVs isolated from HRPEsv cells culture medium by precipitation and differential centrifugation. Sample preparation protocol for TEM using fixation with 4% PFA (w/v) and staining with 2% uranyl acetate (w/v). (A) Precipitation protocol; (B) Differential centrifugation protocol; and (C) Procedural blank by precipitation. White arrow in image A points at a precipitation residue of uranyl acetate salt used for staining.

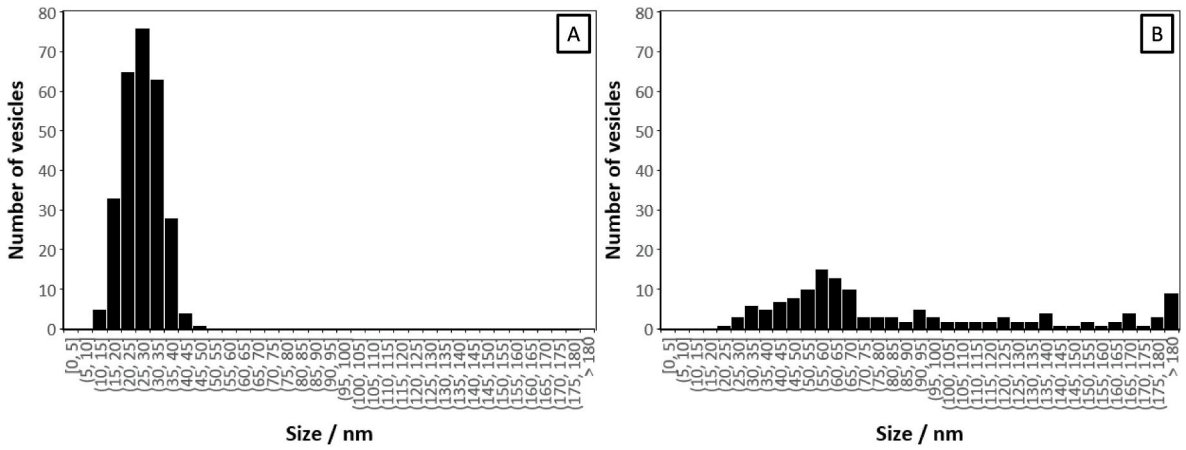

Fig. 2. Size distribution obtained from TEM images (Fig. 1) of exosomes isolated from HRPEsv cells culture medium by using precipitation (panel A) and differential centrifugation purification (panel B) protocols. Each bar displayed in the graph accounts for the number of exosomes found to have a size inside the corresponding five-value Interval. Exosome size was determined as the longer diameter of the EVs (the majority of the vesicles detected present an oval-like shape).

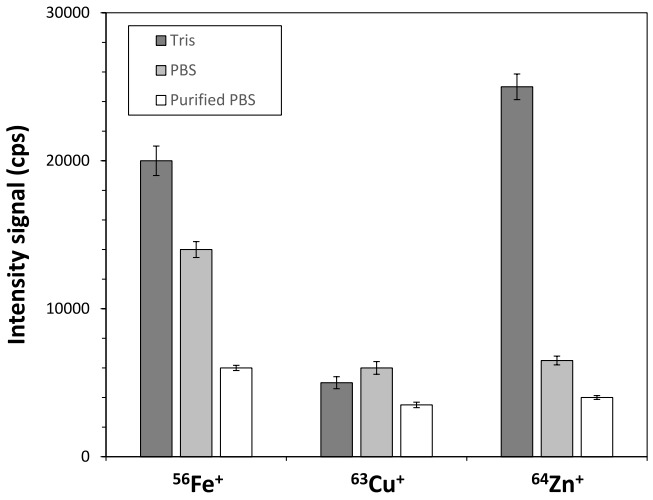

Fig. 3. $^{56}Fe^{+}$, $^{63}Cu^{+}$ and $^{64}Zn^{+}$ intensity signals obtained by ICP-MS for the analysis of different buffers (PBS, purified-PBS and Tris) that can be potentially used for resuspension of exosomes. Uncertainties correspond to the standard deviation value from the mean of three replicates. Sample introduction system: MicroMist.

compared to those observed in PBS. As a consequence of the significant Fe and Zn contamination coming from Tris buffer and taking into account that it is not typically used for EVs analysis, Tris was discarded as buffer for exosomes resuspension. Additionally, as already indicated, TEM images obtained using Tris showed lower resolution and higher aggregation compared to PBS (Fig. S2 and Fig. S1 in Supporting Information, respectively).

Taking into account the low concentration levels expected for endogenous trace elements in the exosomes, it is crucial to reduce as much as possible Fe, Cu and Zn contamination from chemical reagents. Chelex-100, a widely used chelating resin for metals [27], was selected and PBS buffer was treated with the resin to decrease their trace elements content. Hence, 0.2 g of clean dry resin were added to 10 mL solutions and subjected to magnetic stirring for 7 h. Then, the resin was separated by filtration through porous glass and the PBS measured again by ICP-MS (i.e. purified-PBS). The intensity signal obtained for $^{56}Fe^{+}$, $^{63}Cu^{+}$ and $^{64}Zn^{+}$ by ICP-MS analysis of purified-PBS is also collected in Fig. 3: a decrease of Fe, Cu and Zn content was observed after PBS purification. Consequently, purified-PBS was chosen as the most suitable buffer for trace elements determination in exosomes by elemental MS.

On the other hand, three sample introduction systems were evaluated for the determination of Fe, Cu and Zn in exosomes suspensions by ICP-MS: MicroMist, Single Cell and microFAST (optimized experimental parameters for each system are collected in Table 2). The sample flow rate was found to be 66 μL min^{-1}, 33 μL min^{-1} and 17 μL min^{-1} for MicroMist, Single Cell and microFAST, respectively. Challenges associated to the determination of trace elements in exosomes are related not only to the small sample volume available but also to the expected low metals concentration. Thus, the sensitivity provided by the three sample introduction systems was first evaluated in terms of limits of detection (LoDs). External calibration using pure solution standards were performed in the range of 0–20 μg L^{-1} for Fe, Cu and Zn (Ga was selected as internal standard). Calibrations were done, as specified in Section 2.3.6, preparing standards of increasing metals concentration in purified-PBS (diluted 1:5 for precipitation or 1:2 for differential centrifugation to a final concentration of 3% nitric acid and 10 μg L^{-1} Ga). Fig. 4 collects the LoDs obtained for $^{56}Fe^{+}$, $^{63}Cu^{+}$ and $^{64}Zn^{+}$ isotopes using the three systems, calculated as the ratio of three times the standard deviation of

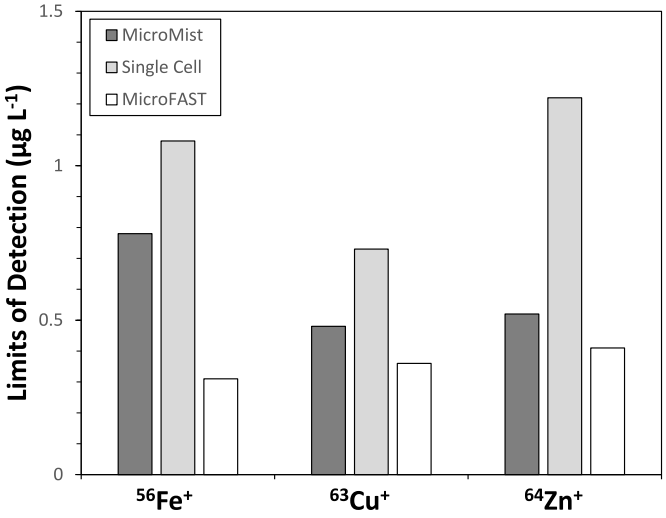

Fig. 4. Limits of detection obtained for $^{56}Fe^{+}$, $^{63}Cu^{+}$ and $^{64}Zn^{+}$ by ICP-MS using three sample introduction systems: MicroMist, Single Cell and microFAST (experimental parameters for each system are collected at Table 2). LoDs were calculated taking into account the calibration graph for each analyte as the ratio of three times the standard deviation of the intercept and the calibration slope.

the intercept and the calibration slope. As it can be seen, the same tendency was observed for $^{56}Fe^{+}$, $^{63}Cu^{+}$ and $^{64}Zn^{+}$: the highest LoDs were found using the Single Cell system, whereas the lowest LoDs were observed with the microFAST system (0.31 μg L^{-1} for $^{56}Fe^{+}$, 0.36 μg L^{-1} for $^{63}Cu^{+}$ and 0.41 μg L^{-1} for $^{64}Zn^{+}$). LoDs reached with the MicroMist and microFAST systems for Cu and Zn were in the same range, whereas the LoD for Fe was significantly better using microFAST (0.78 μg L^{-1} *versus* 0.31 μg L^{-1}). Moreover, as stated above, a significant lower sample uptake rate was provided by the microFAST system compared to MicroMist (17 μL min^{-1} *versus* 66 μL min^{-1}). Therefore, microFAST introduction system (as total consumption set-up) was selected as the optimum for the bulk determination of trace elements in exosomes by ICP-MS.

Here, it should be stated that ICP-MS is an analytical technique offering high sensitivity, specifity, multi-elemental and multi-isotopic capability and a long linear range. Therefore, nowadays it is considered the gold standard for the reliable determination of very low contents of metals in complex biological samples, such as trace elements in exosomes. In this study we have used proper pure standards of the investigated elements for quantification purposes, following well established procedures for calibration. Future studies may consider to establish "reference materials" of exosomes (or EVs) for interlaboratory comparison.

3.2.2. *Determination of Fe, Cu and Zn in exosomes isolated by precipitation and differential centrifugation*

Fe, Cu and Zn concentrations in exosomes isolated from HRPEsv cells culture medium were determined by ICP-MS after the precipitation and differential centrifugation isolation protocols. Three biological replicates (in purified-PBS) and procedural blanks for each isolation protocol were analyzed using microFAST sample introduction system. Procedural blanks (ExoQuick-TC reagent for precipitation and purified-PBS for differential centrifugation together with the culture medium without HRPEsv cells) were measured by ICP-MS to determine their contribution to the sample. As can be seen in Table 3, the metals concentrations in the procedural blanks were significantly higher for precipitation-isolated exosomes as compared to the procedural blanks obtained by differential centrifugation. The serious metals contribution of precipitation procedural blanks can be attributed to the ExoQuick-TC reagent. Thus, although a lower exosomes production is expected by using differential centrifugation for isolation of exosomes from cells culture medium, a lower Fe, Cu and Zn external contamination is also produced. Table 3 also collects the Fe, Cu and Zn concentrations determined in the exosomes samples without blank subtraction (i.e., raw metals concentration).

The average of the blank subtracted metals concentrations for exosomes suspensions are the following: 27 ± 3 μg L^{-1} of Fe, 10 ± 4 μg L^{-1} of Cu and 29 ± 3 μg L^{-1} of Zn for the precipitation-based isolation protocol, while 8.1 ± 0.4 μg L^{-1} of Fe, 2.6 ± 0.3 μg L^{-1} of Cu and 16.7 ± 2 μg L^{-1} of Zn was obtained using the differential centrifugation protocol. As can be observed, Fe, Cu and Zn levels were slightly higher in precipitation-isolated exosomes compared to differential centrifugation (3.3-fold for Fe, 3.8-fold for Cu, and 1.7-fold for Zn). These small differences differ with data obtained by TEM and total protein content, where about a 30-fold higher exosomes concentration was obtained by the precipitation method. To account for the experimental results, it must be kept in mind that particles of smaller size were observed using the precipitation protocol (see Fig. 2). Thus, although exosomes are present in a higher number following the precipitation protocol, small exosomes would have less Fe, Cu and Zn (referring to mass, not to concentration) and therefore, they contribute less to the concentrations determined by ICP-MS with conventional nebulization (i.e., giving the average metals concentration in the bulk population of exosomes).

Taking into account the high contribution of blanks observed by the precipitation method as compared to the raw signals (Table 3 collects the ratio "sample/blank" for both procedures indicated as the fold change) and the fact that the net differences in metal concentrations observed by both methods were rather similar, the differential centrifugation isolation method was selected for further experiments.

Table 3
Fe, Cu and Zn concentrations determined by ICP-MS (microFAST sample introduction system) in exosomes suspensions (Raw) and procedural blanks (Blk) from HRPEsv cells culture medium. In both cases, results were compared for two isolation protocols: precipitation (P) and differential centrifugation (DC). Three biological replicates (R1, R2 and R3) for each isolation protocol were measured and three instrumental replicates were acquired in all cases.

	[Fe] (μg L^{-1})		[Cu] (μg L^{-1})		[Zn] (μg L^{-1})	
Raw P-R1	137 ± 2	139 ± 2	29.1 ± 0.9	22 ± 7	92 ± 2	94 ± 3
Raw P-R2	140 ± 1		19 ± 1		96 ± 2	
Raw P-R3	140 ± 1		18 ± 0.9		92 ± 1	
Blk P-R1	111 ± 1	112 ± 4	14.0 ± 0.4	12 ± 2	62 ± 1	65 ± 4
Blk P-R2	108 ± 2		10.4 ± 0.3		69 ± 2	
Blk P-R3	116 ± 2		10.4 ± 0.2		65 ± 2	
Precipitation Fold change	1.2		1.8		1.4	
Raw DC-R1	15 ± 1	14 ± 3	4.9 ± 0.1	4.1 ± 0.8	22.3 ± 0.8	23 ± 1
Raw DC-R2	14.8 ± 0.9		3.88 ± 0.09		22.3 ± 0.9	
Raw DC-R3	11.0 ± 0.9		3.4 ± 0.1		24 ± 1	
Blk DC-R1	5.8 ± 0.1	5.9 ± 0.4	1.81 ± 0.03	1.5 ± 0.4	6.4 ± 0.1	6.3 ± 0.4
Blk DC-R2	6.4 ± 0.2		1.17 ± 0.03		6.2 ± 0.2	
Blk DC-R3	5.5 ± 0.2		1.43 ± 0.03		6.4 ± 0.2	
D. Centrifugation Fold change	2.3		2.7		3.7	

3.3. *Evaluation of AAPH-induced oxidative stress on metal composition of exosomes isolated from HRPEsv cell cultures*

Once the experimental conditions were optimized in terms of the most appropriate isolation protocol for metals determination in exosomes (differential centrifugation) and the experimental set-up for ICP-MS analysis (exosomes resuspended in purified-PBS and the use of microFAST sample introduction system), changes in trace element composition of exosomes induced by OS conditions have been studied.

Changes in Fe, Cu and Zn concentrations of exosomes from non-treated (or CT) and AAPH-treated HRPEsv cells were investigated. Thus, exosomes isolated from culture medium of CT cells and cells with an AAPH-induced oxidative stress treatment (5 mM AAPH, 24 h) were analyzed by ICP-MS. Three biological replicates for each condition (CT and AAPH-treated) along with three procedural blanks of each condition were analyzed by ICP-MS at the optimized experimental conditions. It should be stated that although the same HRPEsv cell line was always used in this work, different aliquots of the cells population were independently sub-cultured depending on the experiments; thus, small variations on the cell passaging as well as on cells confluence can be found between measurements. In this vein, CT samples used to study the effect of oxidative stress treatment were cultured concurrently to AAPH-treated samples (i.e., exosomes from CT cells were different to those analyzed in previous sections). Table 4 collects the Fe, Cu and Zn concentrations determined in exosomes from culture medium derived of CT and AAPH-treated HRPEsv cells. Such results can be also graphically observed in Fig. S3 (Supporting Information). The total protein content was also determined in the exosomes suspensions, showing similar values for CT and AAPH-treated conditions (10 ± 2 mg L^{-1} for CT and

Table 4
Fe, Cu and Zn concentrations determined by ICP-MS (microFAST sample introduction system) in exosomes, either from control (CT) or from AAPH-treated HRPEsv cells culture medium, isolated by differential centrifugation. Three biological replicates (R1, R2 and R3) were measured for each condition and three instrumental replicates were acquired in all cases. p-values were obtained by unpaired *t*-test. p-value>0.05 not significant; p-value<0.001, extremely significant.

	[Fe] (μg L^{-1})		[Cu] (μg L^{-1})		[Zn] (μg L^{-1})	
CT/R1	3.00 ± 0.03	2.7 ± 0.3	1.30 ± 0.04	1.3 ± 0.3	10.22 ± 0.05	10.9 ± 0.8
CT/R2	2.73 ± 0.04		1.37 ± 0.03		11.55 ± 0.06	
CT/R3	2.34 ± 0.01		1.08 ± 0.03		10.89 ± 0.04	
AAPH-treated/R1	3.4 ± 0.3	3.2 ± 0.4	1.10 ± 0.04	1.2 ± 0.3	34.9 ± 0.3	34 ± 2
AAPH-treated/R2	2.6 ± 0.2		1.37 ± 0.08		37 ± 2	
AAPH-treated/R3	3.5 ± 0.2		0.98 ± 0.05		31.0 ± 0.1	
AAPH vs Control (fold-change, p-value)	1.2-fold, p > 0.05		0.9-fold, p > 0.05		3.1-fold, p < 0.001	

10 ± 3 mg L^{-1} for AAPH-treated) that allow a direct comparison of the metals concentration between the two exosomes-containing samples.

Fe, Cu and Zn levels of exosomes were statistically compared between experimental conditions, i.e., AAPH-treated cells *versus* CT cells. As can be observed in Table 4, Fe and Cu concentrations were not statistically significant different in exosomes derived from CT and AAPH-treated HRPEsv cell culture medium (1.2-fold change and 0.9-fold change, respectively, p-value>0.05 of unpaired *t*-test). Interestingly, Zn levels within exosomes exhibited a statistically significant increase (3.1-fold change, p-value<0.001, unpaired *t*-test) when compared APPH-induced OS conditions with non-treated HRPEsv cells. We previously observed that short term AAPH treatment (5 mM, 1 h) of HRPEsv cells *in vitro* down-regulated the overall levels of Zn-binding proteins [20], which may be related with Zn protection against oxidative stress-induced RPE death [28,29]. Oxidative stress also seems to promote exosome secretion of cultured RPE cells [22], where intracellular reactive oxidative species increase the number of intracellular multivesicular bodies enhancing the release of EVs [30]. Overall, the observed higher levels of Zn in secreted exosomes may be conditional to decreased intracellular Zn levels, which could imply a novel mechanism of cellular Zn depletion warranting further research.

4. Conclusion

This work marks the first time that the levels of endogenous trace elements are successfully determined in exosomes secreted by an *in vitro* cell culture. Different exosomes isolation protocols are described in the bibliography, but no one focuses on their suitability for ICP-MS analysis of the endogenous metal content on isolated EVs. In this work, two of the most used isolation protocols, one based on differential centrifugation and other based on precipitation with ExoQuick-TC, were compared in terms of ICP-MS suitability, to establish an ICP-MS protocol for the multielemental analysis of exosomes. For the purposes of this work, differential centrifugation was chosen as the most suitable isolation method, as it does not have a significant contribution to the ICP-MS blank compared to precipitation blanks. The effectiveness of other exosomes isolation methods widely used, like size exclusion chromatography or immunoaffinity-based methods, are still not proven for ICP-MS analysis, which may be an interesting research to perform in the future.

Zn levels found in exosomes secreted by OS-treated cells remarks the importance of the trace metal homeostasis (especially Zn) in RPE cells and allows to see the response of cells against a stress situation, probably activating their antioxidant mechanisms both through intracellular and secretory activity changes. This study can be extended to exosomes isolated from other biological fluids, such as blood, or to closely eye-related biofluids, like aqueous humor or tears, to evaluate whether disease onset affecting eye tissues alters trace element levels in exosomes from such fluids.

Finally, it must be highlighted that the methodology here developed is of potential application to any study, with cell lines or biological fluid samples, where metal dyshomeostasis is involved. Therefore, this research warrants further research in the future.

Credit author statement

Jaime Martínez-García: Investigation, Methodology, Writing - Original Draft. Beatriz Fernández: Supervision, Conceptulization, Writing - Review & Editing. Ana Álvarez-Barrios: Validation, Review. Lydia Álvarez: Resources, Visualization. Héctor González-Iglesias: Conceptualization. Rosario Pereiro: Supervision, Funding acquisition, Review.

Declaration of competing interest

The authors declare that they have no known competing financial interests or personal relationships that could have appeared to influence the work reported in this paper.

Data availability

Data will be made available on request.

Acknowledgements

This work was financially supported through projects PID2019-107838RB-I00/Agencia Estatal de Investigación (AEI)/10.13039/501100011033) and the PCTI Program of the Government of the Principality of Asturias and FEDER Program of the European Union (No. AYUD/2021/51289). J. Martínez-García acknowledges the "Severo Ochoa" Program Grant with Ref. BP21-041 (Principality of Asturias, Spain). Authors want to acknowledge C. Derrick Quarles Jr. for his support with the microFAST Single Cell system, and the technical support provided by Servicios Científico-Técnicos of the University of Oviedo – Mass Spectrometry and Electron Microscopy Units. The Instituto Oftalmológico Fernández-Vega and Fundación de Investigación Oftalmológica acknowledge financial support from the Fundación Rafael del Pino (http://www.frdelpino.es), through the "Cátedra Rafael del Pino" and from IDE/2019/000289 project of "Instituto de Desarrollo Económico del Principado de Asturias" (IDEPA) of Gobierno del Principado de Asturias and FEDER.

Appendix A. Supplementary data

Supplementary data to this article can be found online at https://doi.org/10.1016/j.talanta.2023.124693.

References

[1] L.M. Doyle, M.Z. Wang, Overview of extracellular vesicles, their origin, composition, purpose, and methods for exosome isolation and analysis, Cells 8 (2019) 727, https://doi.org/10.3390/cells8070727.
[2] J. Ghanam, V.K. Chetty, L. Barthel, D. Reinhardt, P. Hoyer, B.K. Thakur, DNA in extracellular vesicles: from evolution to its current application in health and disease, Cell Biosci. 12 (2022) 37, https://doi.org/10.1186/s13578-022-00771-0.
[3] G. Van Niel, G. D'Angelo, G. Raposo, Shedding light on the cell biology of extracellular vesicles, Nat. Rev. Mol. Cell Biol. 19 (2018) 213–228, https://doi.org/10.1038/nrm.2017.125.
[4] E. Bazzan, M. Tinè, A. Casara, D. Biondini, U. Semenzato, E. Cocconcelli, E. Balestro, M. Damin, C.M. Radu, G. Turato, S. Baraldo, P. Simioni, P. Spagnolo, M. Saetta, M.G. Cosio, Critical review of the evolution of extracellular vesicles' knowledge: from 1946 to today, Int. J. Mol. Sci. 22 (12) (2021) 6417, https://doi.org/10.3390/ijms22126417.

[5] M.Z. Ratajczak, J. Ratajczak, Extracellular microvesicles/exosomes: discovery, disbelief, acceptance, and the future? Leukemia 34 (2020) 3126–3135, https://doi.org/10.1038/s41375-020-01041-z.
[6] M. Battistelli, E. Falcieri, Apoptotic bodies: particular extracellular vesicles involved in intercellular communication, Biology 9 (1) (2020) 21, https://doi.org/10.3390/biology9010021.
[7] I.K. Herrmann, M.J.A. Wood, G. Fuhrmann, Extracellular vesicles as a next-generation drug delivery platform, Nat. Nanotechnol. 16 (2021) 748–759, https://doi.org/10.1038/s41565-021-00931-2.
[8] M.C. Ciferri, R. Quarto, R. Tasso, Extracellular vesicles as biomarkers and therapeutic tools: from pre-clinical to clinical applications, Biology 10 (5) (2021) 359, https://doi.org/10.3390/biology10050359.
[9] Y. Gao, Y. Qin, C. Wan, Y. Sun, J. Meng, J. Huang, Y. Hu, H. Jin, K. Yang, Small extracellular vesicles: a novel avenue for cancer management, Front. Oncol. 11 (2021), 638357, https://doi.org/10.3389/fonc.2021.638357.
[10] M. Harmati, E. Gyukity-Sebestyen, G. Dobra, L. Janovak, I. Dekany, O. Saydam, E. Hunyadi-Gulyas, I. Nagy, A. Farkas, T. Pankotai, Z. Ujfaludi, P. Horvath, F. Piccinini, M. Kovacs, T. Biro, K. Buzas, Small extracellular vesicles convey the stress-induced adaptive responses of melanoma cells, Sci. Rep. 9 (2019), 15329, https://doi.org/10.1038/s41598-019-51778-6.
[11] Y. Gao, X. Huang, H. Lin, M. Zhao, W. Liu, W. Li, L. Han, Q. Ma, C. Dong, Y. Li, Y. Hu, F. Jin, Adipose mesenchymal stem cell-derived antioxidative extracellular vesicles exhibit anti-oxidative stress and immunomodulatory effects under PM2.5 exposure, Toxicology 447 (2021), 152627, https://doi.org/10.1016/j.tox.2020.152627.
[12] M.D. Jelic, A.D. Mandic, S.M. Maricic, B.U. Srdjenovic, Oxidative stress and its role in cancer, J. Cancer Res. Therapeut. 17 (2021) 22–28, https://doi.org/10.4103/jcrt.JCRT_862_16.
[13] A. Singh, R. Kukreti, L. Saso, S. Kukreti, Oxidative stress: a key modulator in neurodegenerative diseases, Molecules 24 (8) (2019) 1583, https://doi.org/10.3390/molecules24081583.
[14] A. Álvarez-Barrios, L. Álvarez, M. García, E. Artime, R. Pereiro, H. González-Iglesias, Antioxidant defenses in the human eye: a focus on metallothioneins, Antioxidants 10 (1) (2021) 89, https://doi.org/10.3390/antiox10010089.
[15] S. Yang, J. Zhou, D. Li, Functions and diseases of the retinal pigment epithelium, Front. Pharmacol. 12 (2021), 727870, https://doi.org/10.3389/fphar.2021.727870.
[16] E.E. Brown, A.J. DeWeerd, C.J. Ildefonso, A.S. Lewin, J.D. Ash, Mitochondrial oxidative stress in the retinal pigment epithelium (RPE) led to metabolic dysfunction in both the RPE and retinal photoreceptors, Redox Biol. 24 (2019), 101201, https://doi.org/10.1016/j.redox.2019.101201.
[17] S.R. Weber, M. Zhou, Y. Zhao, J.M. Sundstrom, Exosomes in retinal diseases, in: Exosomes, a Clinical Compendium, 2020, p. 415–431, https://doi.org/10.1016/B978-0-12-816053-4.00018-3.
[18] M. Flores-Bellver, J. Mighty, S. Aparicio-Domingo, K. Li, C. Shi, H. Cobb, J. Zhou, P. Lenhart, G.A. Michelis, A.E. Goodspeed, S. Heissel, C. Coughlan, S.P. Becerra, S. M. Redenti, V.C. Soler, Drusen proteins are released in association with exosomes, Invest. Ophthalmol. Vis. Sci. 62 (8) (2021) 2225.
[19] R.S. Amais, G.L. Donati, M.A.Z. Arruda, ICP-MS and trace element analysis as tools for better understanding medical conditions, Trends Anal. Chem. 133 (2020), 116094, https://doi.org/10.1016/j.trac.2020.116094.
[20] S. Rodríguez-Menéndez, B. Fernández, M. García, L. Álvarez, M.L. Fernández, A. Sanz-Medel, M. Coca-Prados, R. Pereiro, H. González-Iglesias, Quantitative study of zinc and metallothioneins in the human retina and RPE cells by mass spectrometry-based methodologies, Talanta 178 (2018) 222–230, https://doi.org/10.1016/j.talanta.2017.09.024.
[21] C. Théry, A. Clayton, S. Amigorena, G. Raposo, Isolation and characterization of exosomes from cell culture supernatants and biological fluids, Curr. Prot. Cell Biol. 30 (2006), https://doi.org/10.1002/0471143030.cb0322s30 (Chapter 3): Unit 3.22.
[22] S. Atienzar-Aroca, M. Flores-Bellver, G. Serrano-Heras, N. Martinez-Gil, J. M. Barcia, S. Aparicio, D. Perez-Cremades, J.M. Garcia-Verdugo, M. Diaz-Llopis, F. J. Romero, J. Sancho-Pelluz, Oxidative stress in retinal pigment epithelium cells increases exosome secretion and promotes angiogenesis in endothelial cells, J. Cell Mol. Med. 20 (8) (2016) 1457–1466, https://doi.org/10.1111/jcmm.12834.
[23] L.G. Rikkert, R. Nieuwland, L.W.M.M. Terstappen, F.A.W. Coumans, Quality of extracellular vesicle images by transmission electron microscopy is operator and protocol dependent, J. Extracell. Vesicles 8 (2019), 1555419, https://doi.org/10.1080/20013078.2018.1555419.
[24] M.K. Jung, J.Y. Mun, Sample preparation and imaging of exosomes by transmission electron microscopy, J. Visual. Exp. 131 (2018), 56482, https://doi.org/10.3791/56482.
[25] R. Linares, S. Tan, C. Gounou, N. Arraud, A.R. Brisson, High-speed centrifugation induces aggregation of extracellular vesicles, J. Extracell. Vesicles 4 (2015), 29509, https://doi.org/10.3402/jev.v4.29509.
[26] G. Raposo, W. Stoorvogel, Extracellular vesicles: exosomes, microvesicles, and friends, J. Cell Biol. 200 (4) (2013) 373–383, https://doi.org/10.1083/jcb.201211138.
[27] A.M. Massadeh, A.W.O. El-Rjoob, S.A. Gharaibeh, Analysis of selected heavy metals in tap water by inductively coupled plasma-optical emission spectrometry after pre-concentration using chelex-100 ion exchange resin, Water Air Soil Pollut. 231 (2020) 243, https://doi.org/10.1007/s11270-020-04555-5.
[28] D.J. Tate Jr., M.V. Miceli, D.A. Newsome, Zinc protects against oxidative damage in cultured human retinal pigment epithelial cells, Free Radic. Biol. Med. 26 (1999) 704–713, https://doi.org/10.1016/s0891-5849(98)00253-6.
[29] D. Rajapakse, T. Curtis, M. Chen, H. Xu, Zinc protects oxidative stress-induced RPE death by reducing mitochondrial damage and preventing lysosome rupture, Oxid. Med. Cell. Longev. 2017 (2017), 6926485, https://doi.org/10.1155/2017/6926485.
[30] W. Zhang, R. Liu, Y. Chen, M. Wang, J. Du, Crosstalk between oxidative stress and exosomes, Oxid. Med. Cell. Longev. 2022 (2022), 3553617, https://doi.org/10.1155/2022/3553617.